

Effect of Fe on physical characteristics of CdS: DFT investigations

S. A. Aldaghfag^a, M. Yaseen^{b,*}, H. Ambreen^b, M. K. Butt^b, M. Rehan^b, A. Dahshan^{c,d}

^aDepartment of Physics, College of Sciences, Princess Nourah bint Abdulrahman University (PNU), Riyadh 11671, Saudi Arabia

^bSpin-Optoelectronics and Ferro-Thermoelectric (SOFT) Materials and Devices Laboratory, Department of Physics, University of Agriculture, Faisalabad 38040, Pakistan

^cDepartment of Physics - Faculty of Science - King Khalid University, P.O. Box 9004, Abha, Saudi Arabia

^dDepartment of Physics, Faculty of Science, Port Said University, Port Said, Egypt

In this work, the electronic, magnetic and optical features of the diluted magnetic semiconductors (DMS) $Cd_{1-x}Fe_xS$ ($x= 6.25\%$, 12.5% , 25%) are determined by density functional theory (DFT). The analysis of electronic BS and magnetic moment of $Cd_{1-x}Fe_xS$ show a half metallic ferromagnetic (HMF) nature with direct energy gap (E_g). The E_g of CdS is elevated by incrementing the doping concentration of iron atoms. Moreover, the replacement of Cd with Fe turns CdS into *an*-type semiconductor. The effect of Fe concentration on the optical parameters such as absorption coefficient, refractive index, dielectric function, optical conductivity, and reflectivity is also investigated. Results revealed that $Cd_{1-x}Fe_xS$ is a suitable compound for spintronics and optoelectronics devices.

(Received April 25, 2021; Accepted July 1, 2021)

Keywords: Electronic band structure, Magnetic nature, Optical properties, Spintronics

1. Introduction

Since the two decades, DMSs have been intensively explored because of their enormous technological and scientific applications in various fields especially spin based electronics also called spintronics [1]. In HMF materials, one spin state shows significant E_g around the Fermi level (E_f), however the other spin state demonstrates conducting behavior [2]. In 1983, De Greet *et al.*, in 1983 given the concept of HMF [3]. To find the half metallic dilute ferromagnetic semiconductor with 100% spin polarization is a key challenge for scientist. HMFs have been investigated both experimentally and theoretically (computational) in a variety of compounds that includes metal oxides such as CrO_2 [4], Fe_3O_4 [5], Co_2FeSi [6], Co_2M_nSi [7], double perovskite alloys such as Sr_2FeMoO_6 [8], and $La_{0.7}S_{0.3}M_nO_3$ [9].

Cadmium sulfide is a significant semiconductor with 2.42 eV E_g at the room temperature. Cadmium Sulphide (CdS) has hexagonal lattice structure at the ambient pressure and temperature [10]. Iron (Fe) behave as a good ferromagnetic material (FM) with high Curie temperature and low coercivity. Fe doped Cadmium sulfide have wide band gap, which can be controlled by changing the Fe concentration [11]. The knowledge of transition metal doped compounds is necessary to fabricate the electronic gadgets like, ultra-fast optical switches, spin valves, logic devices and magnetic sensors. Diluted magnetic semiconductors (DMSs) have been utilized to create the HMF such as Cr-doped MgS, Fe doped CdS and Co and V doped CdS [12].

In the current computational work, we explored the electronic, optical and magnetic characteristics of low concentration Fe doped CdS. The transition metal like iron is employed as a doping material to enhance the spin polarization in CdS compound.

* Corresponding author: myaseen_taha@yahoo.com
KWWSVGRLRUJ&

2. Method of calculation

An ab initio calculations were used to calculate the properties of HMF material, by employing WIEN2K code. The exchange-correlation potential of system and relativistic effect in scalar approximation was measured by PBEsol+GGA. CdS has face centered cubic (FCC) structure and Cd occupy position (0, 0, 0) and S (0.25, 0.25, 0.25). In these calculations, Fe(3d⁶,4s²), Cd(4d¹⁰,5s²) and S(3s²,3p⁴) are considered as outer states and the other states are taken as core states [13]. The chosen muffin-tin radii for crystal potential are 2.43 a.u. for Fe and Cd and 2.43 a.u. for S.35 k point meshes were used to calculate the charge density, smooth part of potential and wave function. The parameter $R_{\min}K_{\max}$ is chosen as 7.5 to control the size of basis set in our calculations. A plane wave cutoff energy 350 eV is selected. In order to determine the density of states, the tetrahedron method of the first Brillouin zone (BZ) integration was used. To achieve the self-consistency of system, the energy difference was always less than the 10⁵ per formula unit between consequent iterations. In CdS crystal system, the Cd atom is replaced by Fe to get the ordered structure [14]. The Iron doped Cadmium sulfide (CdS) structure is optimized to get the lattice constants.

3. Results and discussions

3.1. Electronic properties

The spin-dependent band diagram of Cd_{1-x}Fe_xS (x = 6.25%, 12.5%, 25%) in the first BZ is shown in Fig. 1. The obtained results indicate a huge exchange spin splitting between the minority and majority spins states around the Fermi region. It indicates the origin of magnetism in the host material because of the doping of TM (Fe) atoms. Spin-up channel show the semiconductor behavior while the spin-dn show the metallic properties due to the overlapping of Fermi level. It can also be observed that CB (bottom) and VB (top) are located at Γ point of first BZ, which indicates a direct E_g in Fe doped CdS. The BS of Cd_{1-x}Fe_xS (x = 6.25%, 12.5%, 25%) compounds in its ferromagnetic states exhibits half metallic (HM) behavior. The band introduced by dopants occupy the energy level below the CB of host compound, which indicates the conversion of CdS into *n*-type semiconductor. The calculated HM gap and the E_g for pure and Fe doped CdS compounds are given in Table 1. Clearly, the HM gap and E_ggap in spin-up state become larger when the concentration of Fe increases up to x = 25%.HM gap is considered an essential parameter for spintronics devices [15].

The TDOS, PDOS and the electronic BS for Cd_{1-x}Fe_xS (x = 6.25%, 12.5%, 25%) are investigated to get the deeper knowledge about the contribution of each orbit of an atom. The outcomes are illustrated in Fig. 2-5. The first observation is the spin polarization between spin-dn and spin-up DOS. At Fermi level, the spin polarization of Cd_{1-x}Fe_xS compound is represented with the given equation [16]

$$P = \frac{N^{\uparrow}(E_F) - N^{\downarrow}(E_F)}{N^{\uparrow}(E_F) + N^{\downarrow}(E_F)} \quad (1)$$

The DOS graphs shows that Fe doped CdS compound show HMF behavior, because the spin-dn state act as metallic and spin-up as semiconductor with 100% spin polarization around the Fermi level. The *d* electrons of iron are the major factor for magnetic state and localized on the doped site of CdS [17].The PDOS at 6.25%, 12.5% and 25% concentration, the lower part of the VB is in the span -7.6 to -7.9 eV is populated with Cd-*d* states with very minor role of *s* and *p* states of S and middle part in the span -3 to -6 eV is originated due to S-*p*, Cd-*d* and Fe-*d* states as shown in Fig. 2-4.

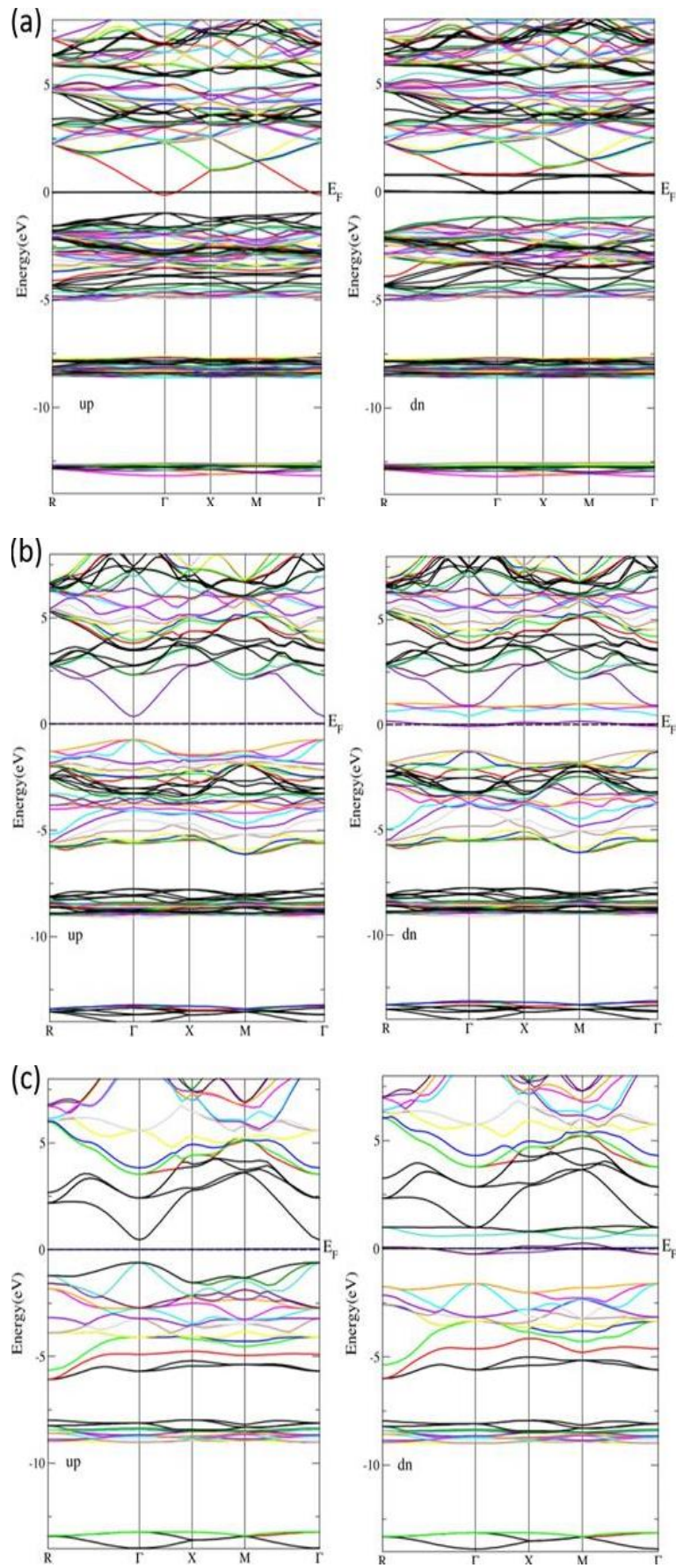


Fig.1. Spin-dependent E_g plot of (a) $Cd_{0.9375}Fe_{0.0625}S$, (b) $Cd_{0.875}Fe_{0.125}S$ (c) $Cd_{0.75}Fe_{0.25}S$.

In Fig.2(c), a significant hybridization taken place between S-*p* states and Fe-*d* states around Fermi level in spin-dn version at $x = 6.25\%$ concentration. At $x=12.5\%$, the HM gap is because of significant hybridization of the Fe-*d* and S-*p* that take part around the Fermi region as indicated in Fig. 3(c) and hybridization at 25% concentration is due to the Fe-*d*, Cd-*d*, S-*p* and S-*s* states as represented in Fig.4(c).

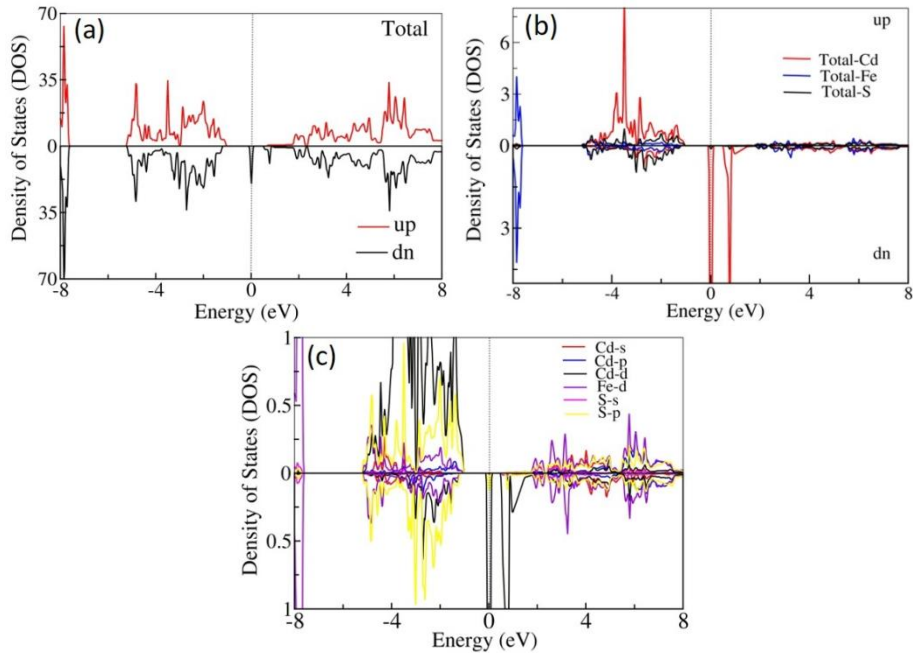


Fig.2. (a & b). Spin-dependent TDOS (c) PDOS of $\text{Cd}_{1-x}\text{Fe}_x\text{S}$ ($x = 6.25\%$).

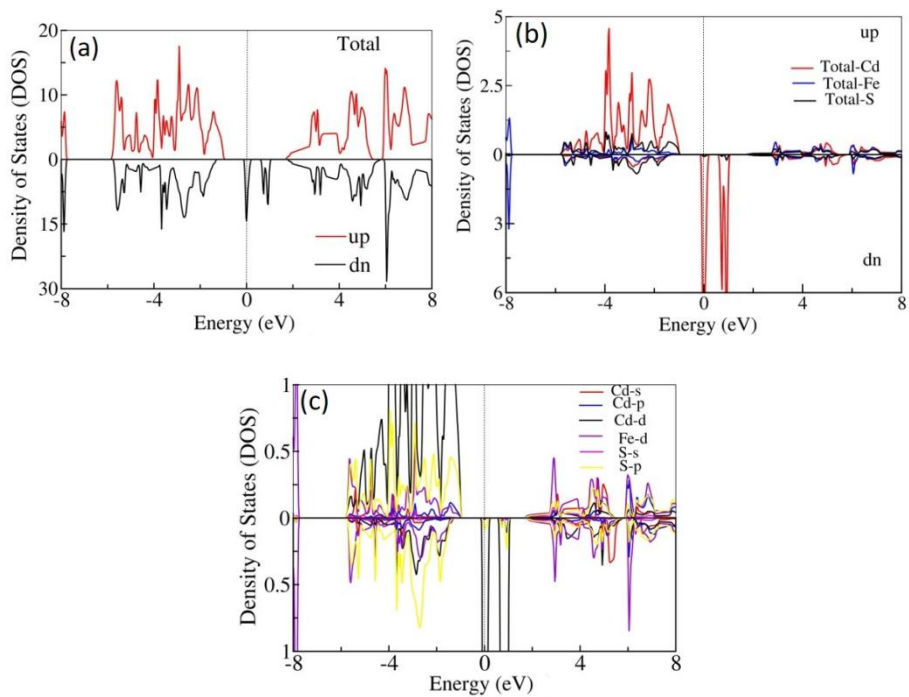


Fig.3. (a & b). Spin-dependent TDOS (c) PDOS of $\text{Cd}_{1-x}\text{Fe}_x\text{S}$ ($x = 12.5\%$).

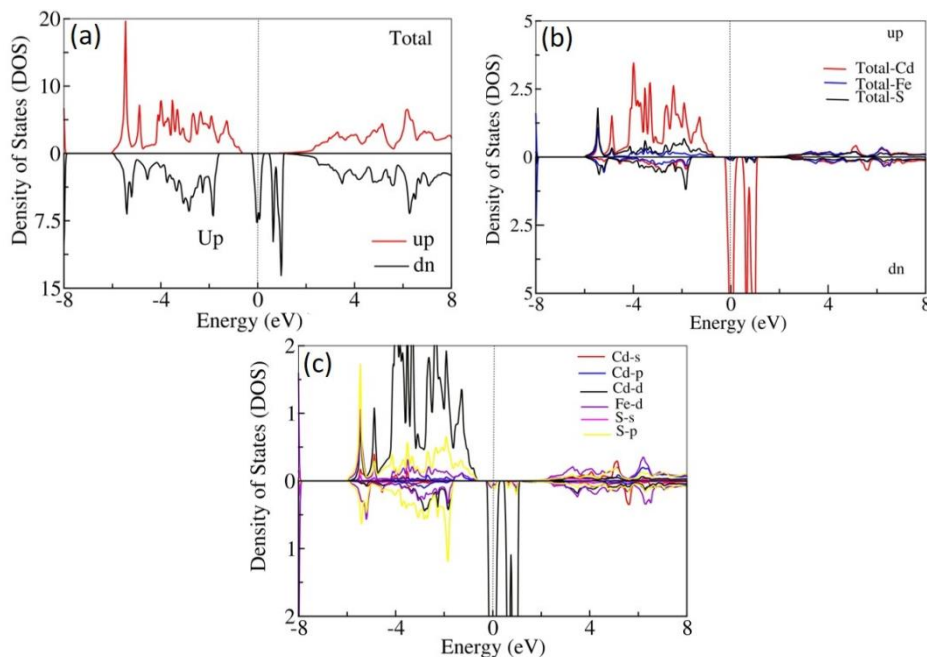


Fig.4. (a & b). Spin-dependent TDOS (c) PDOS of $Cd_{1-x}Fe_xS$ ($x = 25\%$).

3.2. Optical characteristics

Optical features of semiconductors are important to find their significant applications in industry and optical appliances. These properties not only carry the information about the character of the bands but also about the unoccupied and occupied states of electronic structure. All optical constants are derived from $\epsilon_2(\omega)$ and $\epsilon_1(\omega)$ [18]. Optical absorption spectrum can be utilized to obtain the optical features of the compound. The capability of the material for light absorption is checked by $\alpha(\omega)$. The $\alpha(\omega)$ preliminary based on the wavelength of light that is being absorbed in material. The values of absorption peaks are 150, 141 and 168 for $Cd_{0.9375}Fe_{0.0625}S$, $Cd_{0.875}Fe_{0.1250}S$ and $Cd_{0.75}Fe_{0.25}S$, respectively, as depicted in Fig.5(a). The highest absorption curves occurred in the span of ultraviolet region.

In optical properties, the optical conductivity refers to the breaking of bonds when highly energetic electromagnetic waves strike with the material. At $x = 25\%$, the highest peak of optical conductivity occurs at 7.2 eV having magnitude 7000 and smallest peak are seen at low concentrations. After some fluctuations, the optical conductivity decreases for iron doped CdS compounds and turn out to be zero at highest energy values. The highest peaks of optical conductivity occur in the ultra violet (UV) region as represented in Fig.5(b).

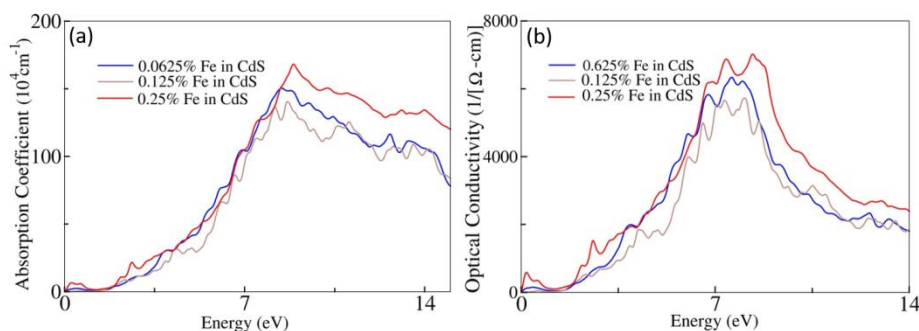


Fig.5. (a) $\alpha(\omega)$ (b) $\sigma(\omega)$ of $Cd_{1-x}Fe_xS$ ($x = 6.25\%, 12.5\%, 25\%$).

$\sigma(\omega)$ and $\alpha(\omega)$ are determined from the following relations [19]

$$I(\omega) = \frac{4\pi}{\lambda} \left(\frac{[\varepsilon_1^2(\omega) + \varepsilon_2^2(\omega)]^{\frac{1}{2}} + \varepsilon_1(\omega)}{2} \right)^{1/2} \quad (2)$$

$$\sigma(\omega) = \frac{\omega}{4\pi} \varepsilon_2(\omega) \quad (3)$$

Complex refractive is shown in Fig. 6. The $n(\omega)$ is basically a complex number that defines how radiations and light are propagated through the material.

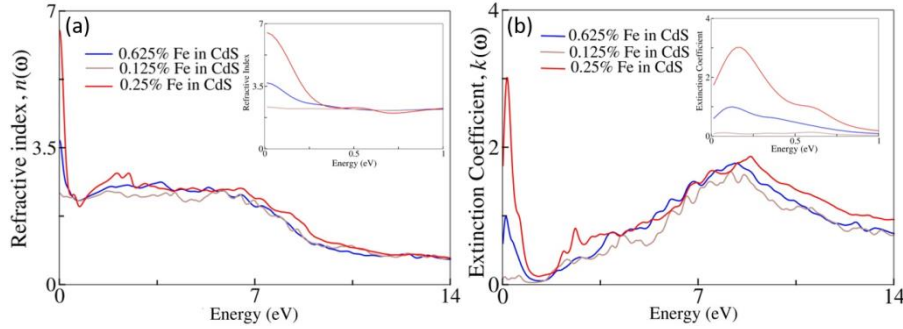


Fig.6. (a) $n(\omega)$ (b) $k(\omega)$ of $Cd_{1-x}Fe_xS$ ($x = 6.25\%, 12.5\%, 25\%$).

The $n(\omega)$ can be represented as:

$$n = \hat{n}(\omega) + ik(\varepsilon) \quad (4)$$

Here n represents the real part and k is the imaginary part for refractive index. $n(\omega)$ and $k(\omega)$ are calculated from the given formulae [20]

$$n(\omega) = \left(\frac{[\varepsilon_1^2(\omega) + \varepsilon_2^2(\omega)]^{\frac{1}{2}} + \varepsilon_1(\omega)}{2} \right)^{1/2} \quad (5)$$

$$k(\omega) = \frac{\alpha\lambda}{4\pi} \quad (6)$$

From 0 to 7 eV, $n(\omega)$ decreases but initially $k(\omega)$ increases and then decreases latter. After 7 eV, k decreases to zero but n become constant which shows that at high frequency CdS has low absorption. The static refractive index for intrinsic CdS is equal to 2.3 which agree with the experimental value 2.43[21]. The following relation is used to relate static dielectric constant with static refractive index $n(0)$:

$$n(0) = \sqrt{\varepsilon(0)} \quad (7)$$

The value of $n(0)$ is 3.7, 2.37 and 6.5 for $Cd_{0.9375}Fe_{0.0625}S$, $Cd_{0.875}Fe_{0.125}S$ and $Cd_{0.75}Fe_{0.25}S$, respectively, which show that $n(0)$ for doped CdS become bigger in comparison with pure CdS as shown in Fig.6(a). The reflectivity of Fe doped CdS compound is determined by using this formula [22]:

$$R(\omega) = \frac{[n(\omega) - 1]^2 + k^2(\omega)}{[n(\omega) + 1]^2 + k^2(\omega)} \quad (8)$$

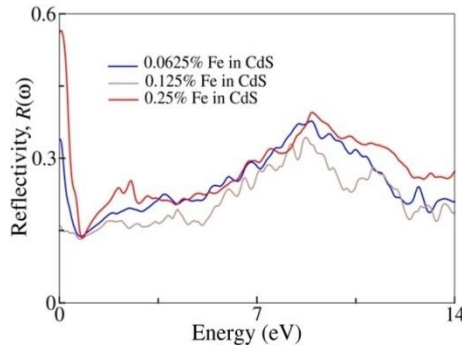


Fig.7. $R(\omega)$ of $Cd_{1-x}Fe_xS$ ($x = 6.25\%$, 12.5% , 25%).

The dielectric function $\varepsilon(\omega)$ is the most important factor, which properly describes the absorption property and polarization of a material. It is given by relation [23]

$$\varepsilon(\omega) = \varepsilon_1(\omega) + i\varepsilon_2(\omega) \quad (9)$$

The complex dielectric function is mainly act as a bridge amongst the electronic BS and inter-band transition [24]. The transition from valance to conduction bands plays a significant role in dielectric properties. The Fig.8 represents the calculated results of $\varepsilon_2(\omega)$ and $\varepsilon_1(\omega)$ for Fe doped CdS. The peaks at low energy appeared in real and imaginary dielectric function due to the doping of TM.

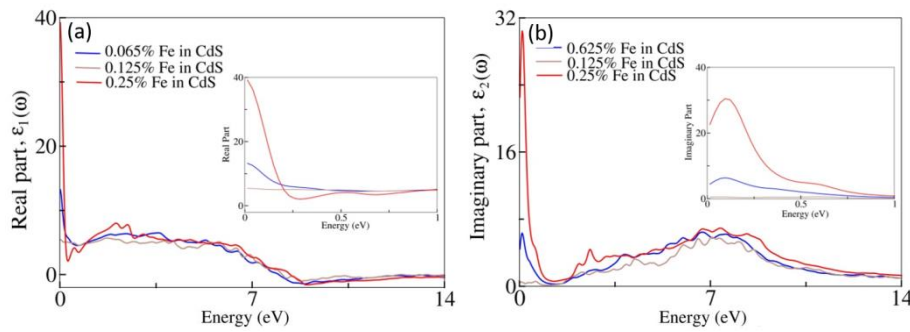


Fig. 8. (a) $\varepsilon_1(\omega)$ (b) $\varepsilon_2(\omega)$ of $Cd_{1-x}Fe_xS$ ($x = 6.25\%$, 12.5% , 25%).

The static dielectric constants $\varepsilon_1(0)$ obtained for $Cd_{0.9375}Fe_{0.0625}S$, $Cd_{0.875}Fe_{0.1250}S$ and $Cd_{0.75}Fe_{0.25}S$ are 13.6, 5.5 and 3.9, respectively, as explained in Fig. 8 (a). The light absorption in material is expressed by $\varepsilon_2(\omega)$. The peaks of spectra are at 6.5, 3.9, 5.8 and 6.7 eV for $Cd_{0.9375}Fe_{0.0625}S$; 3.3, 5.1, 5.7 and 5.9 eV for $Cd_{0.875}Fe_{0.1250}S$; and 3.0, 4.4, 6.2, and 7.6 eV for $Cd_{0.75}Fe_{0.25}S$, respectively, as shown in Fig. 8 (b). The peaks of (ε_2) are direct associated to various interior intra-band transitions in first irreducible BZ [25]. The following formula was used to calculate the imaginary dielectric constant [26];

$$\varepsilon_2(\omega) = \frac{Ve^2}{2\pi\hbar m^2 \omega^2} \int d^3k \sum_{nm'} | \langle kn | p | kn' \rangle |^2 f(kn) \times (1 - f(kn')) \delta(E_{kn} - E_{kn'} - \hbar\omega) \quad (9)$$

The energy of dielectric and absorption peaks are slightly different because of relaxation effect in the electronic transition when the $\alpha(\omega)$ is calculated [27].

3.3. Magnetic properties

The total and local magnetic moments for $\text{Cd}_{1-x}\text{Fe}_x\text{S}$ ($x = 6.25\%$, 12.5% , 25%) are listed in Table-1. The value of Fe concentration cannot be ignored, because the magnetic properties are largely affected by Fe atoms [28]. The partial magnetic moment of Fe is $3.46573 \mu_B$, $3.37118 \mu_B$ and $3.37726 \mu_B$ for $\text{Cd}_{0.9375}\text{Fe}_{0.0625}\text{S}$, $\text{Cd}_{0.875}\text{Fe}_{0.1250}\text{S}$ and $\text{Cd}_{0.75}\text{Fe}_{0.25}\text{S}$ respectively, which confirm the major contribution of Fe in the magnetic moment of CdS compound. The TM doped compounds must have larger magnetic moment due to partially filled 3d orbit, hence they contribute a major role in magnetic characteristics of semiconductors. The transition metal such as Fe behaves as acceptors and possesses states near Fermi-level [29].

Table 1. Calculated energy gaps (E_g), half-metallic gaps (HM), total, Interstitial and Local magnetic moment for $\text{Cd}_{1-x}\text{Fe}_x\text{S}$ ($x = 6.25\%$, 12.5% , 25%).

Compound	E_g (eV)	G_{HM} (eV)	Magnetic Moment (μ_B)				
			Total	Int	Cd	Fe	S
CdS Ref. [29]	0.8	-	-	-	-	-	-
$\text{Cd}_{0.9375}\text{Fe}_{0.0625}\text{S}$	0.8	0	4.00020	0.29187	0.05251	3.46573	0.0495
$\text{Cd}_{0.875}\text{Fe}_{0.1250}\text{S}$	0.97	0.3	4.00000	0.30344	0.08158	3.37118	0.0124
$\text{Cd}_{0.75}\text{Fe}_{0.25}\text{S}$	0.99	0.4	3.99988	0.30031	0.01750	3.37726	0.06745

4. Conclusions

In this paper, electronic behavior, optical and magnetic characteristics at various concentration of Fe-doped CdS compound are investigated by using the DFT method. BS and DOS plots show that $\text{Cd}_{1-x}\text{Fe}_x\text{S}$ ($x = 6.25\%$, 12.5% , 25%) are HMF. It has been found that the band gap increases in spin-up version with the rise of Fe concentration. The estimated E_g of the pure CdS compound is 0.75 eV and it becomes 0.8 eV at 6.25% and 0.99 eV at 25% concentration of Fe. In optical characteristics, we have discussed the $\alpha(\omega)$, dielectric function, $\sigma(\omega)$, $n(\omega)$ and $R(\omega)$ in detail. The alteration in magnetic moment because of Fe doping atoms in CdS is also determined. The results suggest the use of Fe doped CdS compound in spintronics devices due to large magnetic moment and HM behavior.

Acknowledgements

1. This research was funded by the Deanship of Scientific Research at Princess Nourah bint Abdulrahman University through the Fast-track Research Funding Program.
2. The author (A. Dahshan) gratefully thank the Deanship of Scientific Research at King Khalid University for the financial support through research groups program under grant number (R.G.P.2/113/41).

References

- [1] H. M. Gous, A. Meddour, Bourouis, Journal of magnetism and magnetic materials **422**, 271(2017).
- [2] W. E. Pickett, J.S.Moodera, Physics Today **54**,39(2001).
- [3] R. A. De Groot, F. M. Mueller, P. G. van Engen, K. H.J.Buschow, Physical Review Letters **50**, 2024(1983).
- [4] K.L.Yao, G. Y. Gao, Z. L. Liu, L. Zhu, Y. L. Li, Physica B: Condensed Matter **366**, 62(2005).
- [5] S.P.Lewis, P. B. Allen, T. Sasaki, Physical Review **B55**,513(1997).

- [6] I. Galanakis, *Physical Review B* **71**, 012413 (2005).
- [7] S. Wurmehl, G. H. Fecher, H. C. Kandpal, V. Ksenofontov, C. Felser, H. J. Lin, *Applied Physics Letters* **88**, 032503 (2006).
- [8] R. J. Soulen, J. M. Byers, M. S. Osofsky, B. Nadgorny, T. Ambrose, S. F. Cheng, B. Barry, *Science* **282**, 85 (1998).
- [9] K. I. Kobayashi, T. Kimura, H. Sawada, K. Terakura, Y. Tokura, *Nature* **395**, 677 (1998).
- [10] B. O. Seraphin, *Solid-state Phy. Aspect* **41**, 326 (1979).
- [11] K. W. Liu, J. Y. Zhang, D. Z. Shen, B. H. Li, X. J. Wu, B. S. Li, X. W. Fan, *Thin Solid Films* **515**, 8017 (2007).
- [12] T. Nagai, Y. Kanemitsu, M. Ando, T. Kushida, S. Nakamura, Y. Yamada T. Taguchi, *Physica Status Solidi B* **229**, 611 (2002).
- [13] C. Bourouis, A. Meddour, *Journal of magnetism and magnetic materials* **324**, 1040 (2012).
- [14] D. Bimberg, R. Blachnik, M. Cardona, P. J. Dean, T. Grave, G. Harbeke, W. von Münch, *New Series* **17**, 36 (1982).
- [15] G. Y. Gao, K. L. Yao, *Applied Physics Letters* **91**, 082512 (2007).
- [16] K. Kaur, G. S. Lotey, N. K. Verma, *Journal of Materials Science* **25**, 2605 (2014).
- [17] W. Benstaali, S. Bentata, A. Abbad, A. Belaidi, *Materials Science in Semiconductor Processing* **16**, 231 (2013).
- [18] D. E. Aimouch, S. Meskine, A. Birsan, V. Kuncser, A. Zaoui, A. Boukortt, *Materials Chemistry and Physics* **213**, 249 (2018).
- [19] N. A. Noor, N. Ikram, S. Ali, S. Nazir, S. M. Alay-e-Abbas, A. Shaukat, *Journal of Alloys and Compounds* **507**, 256 (2010).
- [20] T. Tsafack, E. Piccinini, B. S. Lee, E. Pop, M. Rudan, *Journal of Applied Physics* **110**, 63761 (2011).
- [21] Y. X. Han, C. L. Yang, Y. T. Sun, M. S. Wang, X. G. Ma, *Journal of Alloys and Compounds* **585**, 503 (2014).
- [22] N. Ullah, G. Murtaza, R. Khenata, J. Rehman, H. U. Din, S. B. Omran, *Materials Science in Semiconductor Processing* **26**, 681 (2014).
- [23] A. Slassi, *Materials Science in Semiconductor Processing* **32**, 100 (2015).
- [24] T. Tsafack, E. Piccinini, B. S. Lee, E. Pop, M. Rudan, *Journal of Applied Physics* **110**, 63716 (2011).
- [25] J. H. Tian, T. Song, X. W. Sun, T. Wang, G. Jiang, *Journal of Superconductivity and Novel Magnetism* **30**, 521 (2017).
- [26] K. Kaur, G. S. Lotey, N. K. Verma, *Journal of Materials Science: Materials in Electronics* **25**, 2605 (2014).
- [27] M. Nakaya, I. Tanaka, A. Muramatsu, *Journal of Nanoscience and Nanotechnology* **12**, 9003 (2012).
- [28] K. A. Bogle, S. Ghosh, S. D. Dhole, V. N. Bhoraskar, L. F. Fu, M. F. Chi, S. B. Ogale, *Journal of Chemistry of materials* **20**, 440 (2007).
- [29] M. Yaseen, H. Ambreen, M. Zia et al., *Journal of Superconductivity and Novel Materials* **34**, 135 (2021).